

Antithyroid Drug Analogues Synthesis and Structural Study

Ms. Ipsita Nath

A Dissertation Submitted to
Indian Institute of Technology Hyderabad
In Partial Fulfillment of the Requirements for
The Degree of Master of Science



भारतीय प्रौद्योगिकी संस्थान हैदराबाद
Indian Institute of Technology Hyderabad

Department of Chemistry

IIT Hyderabad, India

April, 2014

Declaration

I declare that this written submission represents my ideas in my own words, and where others' ideas or words have been included, I have adequately cited and referenced the original sources. I also declare that I have adhered to all principles of academic honesty and integrity and have not misrepresented or fabricated or falsified any idea/data/fact/source in my submission. I understand that any violation of the above will be a cause for disciplinary action by the Institute and can also evoke penal action from the sources that have thus not been properly cited, or from whom proper permission has not been taken when needed.

Ipsita Nath

(- IPSITA NATH -)

(CY12M1009@iith.ac.in)

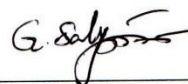
Approval Sheet

This thesis entitled “**Antithyroid Drug Analogues Synthesis and Structural Study**” by Ipsita Nath is approved for the degree of Master of Science from IIT Hyderabad.



-Name and affiliation-

Examiner



-Name and affiliation-

Examiner

Dr. G. Prabusankar
Assistant Professor
Department of Chemistry
Indian Institute of Technology Hyderabad
Ordnance Factory Estate
Yeddumailaram-502 205
Andhra Pradesh, India



-Name and affiliation-

Adviser



-Name and affiliation-

Co-Adviser



-Name and affiliation-

Chairman

Acknowledgements

My sincere thanks to my supervisor Dr. G Prabusankar for his constant support and encouragement, Department of Chemistry, IIT Hyderabad, my seniors in the laboratory for giving me good working experience.

Dedicated to

My Parents and Sister

Abstract

Thiourea-based Antithyroid drugs propylthiouracil (PTU), methimazole (MMI), and carbimazole (CBZ) may block the thyroid hormone biosynthesis whereas selenourea containing drugs reduce H_2O_2 , which is required for oxidation of catalyst leads to decrease in thyroid hormone production. Thus, new tris organo selone derivatives 3,3',3''-((2,4,6-trimethylbenzene-1,3,5-triyl)tris(methylene))tris(1-(2,6-alkyl/aryl)-1H-imidazole-2(3H)-selenone) **4a-4f** have been synthesized for the first time by the reaction of 1,1',1''-((2,4,6-trimethylbenzene-1,3,5-triyl)tris(methylene))tris(3-alkyl/aryl-1H-imidazol-3-ium)bromide (1eq.), potassium carbonate (6eq.) and selenium powder (6eq.). These new molecules have been characterized by multinuclear NMR (1H NMR, ^{13}C NMR, DEPT), FT-IR and UV-vis. studies. The 1H and ^{13}C chemical shifts have been confirmed on the basis of correlation spectra e.g HSQC, HMBC. Photophysical properties have been derived from UV-vis. The molecular structures of **4a**, **4b**, **4c**, **4d** and **4e** have been determined by X-ray crystallography, which suggests that these compounds exist as zwitterions in which the selenium atom carries a large negative charge which enhances the nucleophilic activity of compounds.

Contents

Declaration	2
Approval Sheet	3
Acknowledgements	4
Dedication	5
Abstract	6
Content	7
Chapter 1	
1 Introduction.....	8
1.1 Thyroid hormone synthesis.....	8-9
1.2 Antithyroid drugs.....	9
1.2.1 Thiourea based antithyroid drugs.....	10
1.2.2 Selenourea based antithyroid drugs.....	10-11
1.2.2.1 Mono selones.....	10
1.2.2.2 Bis selones.....	11
2 Aim of work	12
2.1 Target molecules.....	12-14
3 Experimental section	15-19
4 Scheme	20
5 Results and discussion	21-35
6 Conclusion	35
7 Reference	36-37

Chapter 1

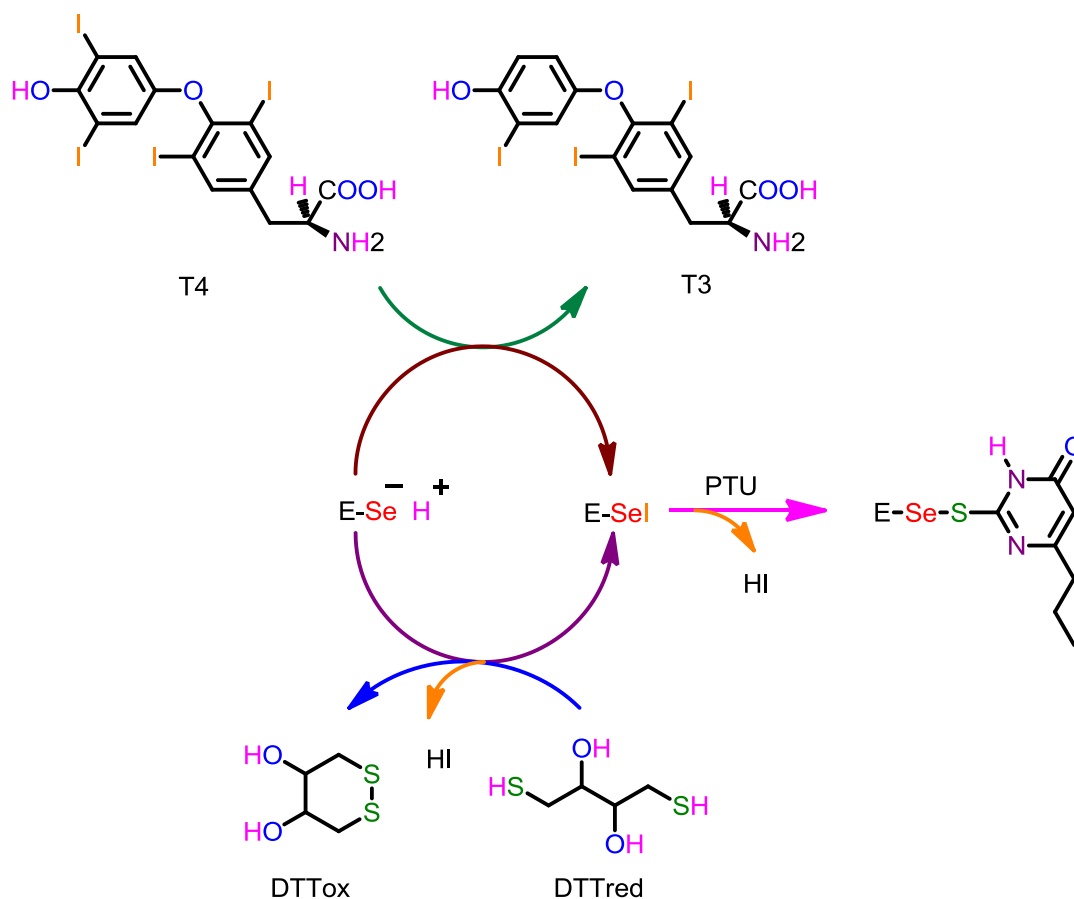
1. Introduction

Organo Imidazolones have been subjected in various applications, such as in metalbased chemistry as a ligands,^[1] preparation of the metal selenides for the use of material chemistry,^[2] and mainly used as antithyroid drugs^[3].

1.1. Thyroid hormone synthesis

Thyroid hormones play an important role in protein, fat, carbohydrate metabolism and cell growth ^[4]. Thyroid hormone secreted from thyroid gland are iodine-containing compounds that control the metabolic rate in every type of tissue the body. Thyroxine (**T4**), the main secretory hormone of the thyroid gland, is produced from thyroglobulin by thyroid peroxidase (TPO)/hydrogen peroxide/iodide system. Biologically active form of prohormone **T4** is **T3** which converts by a selenium-containing iodothyronine deiodinase

(ID-I), mostly exists in liver, kidney, thyroid and pituitary. This deiodination process is catalyzed by ID-I where the selenol (or selenolate) group of the enzyme (E-SeH or E-Se-) first reacts with thyroxine (**T4**) to form a selenenyl iodide (E-SeI) intermediate subsequently E-SeI completes the catalytic cycle and regenerates the selenol by intracellular cofactor (1,4-dithiothreitol (DTT, *Cleland's reagent*) in vitro) (Scheme 1).^[4]



Scheme 1. Mechanism for the Deiodination of Thyroxine by ID-I and Inhibition of ID-I by (PTU)

Autoantibodies causes activation of thyroid stimulating hormone (TSH) receptor leads to an overproduction of thyroid hormones. These antibodies stimulate ID-I and produce relatively more **T3** causing uncontrolled production of thyroid hormones leads to a condition called “hyperthyroidism”^[5].

1.2. Antithyroid drugs

The overproduction of thyroid hormones can be controlled by specific inhibitors, called antithyroid drugs. These are mainly thiourea or selenourea based compounds.

1.2.1. Thiourea based antithyroid drugs ^[6]

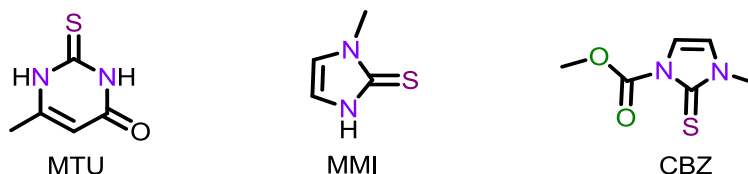


Figure 1. Chemical structures of thiourea based antithyroid drugs

Detailed mechanistic study shows that thiourea-based antithyroid drugs may block the thyroid hormone biosynthesis in vivo by inhibiting TPO-catalyzed iodination of L-tyrosine in which it coordinate with TPO-Fe(III) center ^[7]. Also it has been reported that the selenenyl iodide intermediate (E-SeI) reacts with PTU forming selenenyl sulfide destroying the catalytic enzyme at monodeiodination reaction, hence the conversion of **T4** to **T3** is blocked ^[8].

1.2.2. Selenourea based antithyroid drugs

In contrast to thiourea based drugs, it does not interfere with the native enzyme directly rather inhibits the enzyme activity by reducing the H_2O_2 , which is required for the synthesis of thyroid hormone ^[9] thus it does not block the enzyme (**Scheme 1**). Selenium based antithyroid drugs exists in zwitterionic form where selenium carries the negative charge this leads to higher activity of selenium based drugs than that of sulfur based ^[10].

1.2.2.1. Mono selones ^[11]

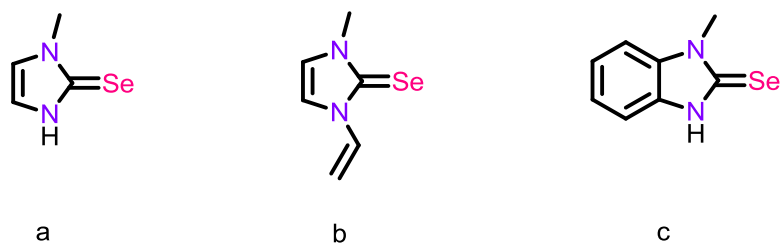


Figure 2. Chemical structures of mono selnoes

1.2.2.2. Bis selones ^[12]

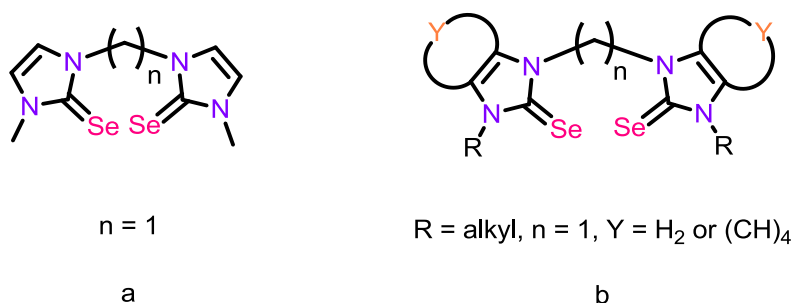


Figure 3. Chemical structures of bis selones

'**Hyperthyroidism**', referred to an **overactive thyroid**, it is a condition where thyroid gland produces and secretes excessive amounts of the thyroid hormones. This is the opposite of hypothyroidism, in which production and secretion of **T₃** and/or **T₄** (i.e. thyroid hormones) reduced. Thyroid hormone is very important for our body, affecting metabolic rate nearly every type of tissue in the body.

If there is excess thyroid hormone, every function of our body tends to speed up as a result some of the symptoms i.e. nervousness, irritability, heart racing, anxiety and muscular weakness. 'Graves' disease is the most common in hyperthyroidism, the eyes may look enlarged because the eye muscles swell and push the eye forward.

Antithyroid drugs may inhibit the overproduction of thyroid hormones antithyroid drugs are mainly thiourea based or selenourea based compounds which prevent the conversion of thyroid hormone **T₄** to the active form **T₃**.

Thiourea and selenourea derivatives inhibit thyroid hormone synthesis by completely different mechanism. Selenourea containing drugs reduce H₂O₂ which is required for oxidation of catalyst leads to

decrease in thyroid hormone production ^[10] whereas Thiourea based drugs probably react with enzyme intermediates which can block hormone synthesis acting as irreversible inhibitor ^[13].

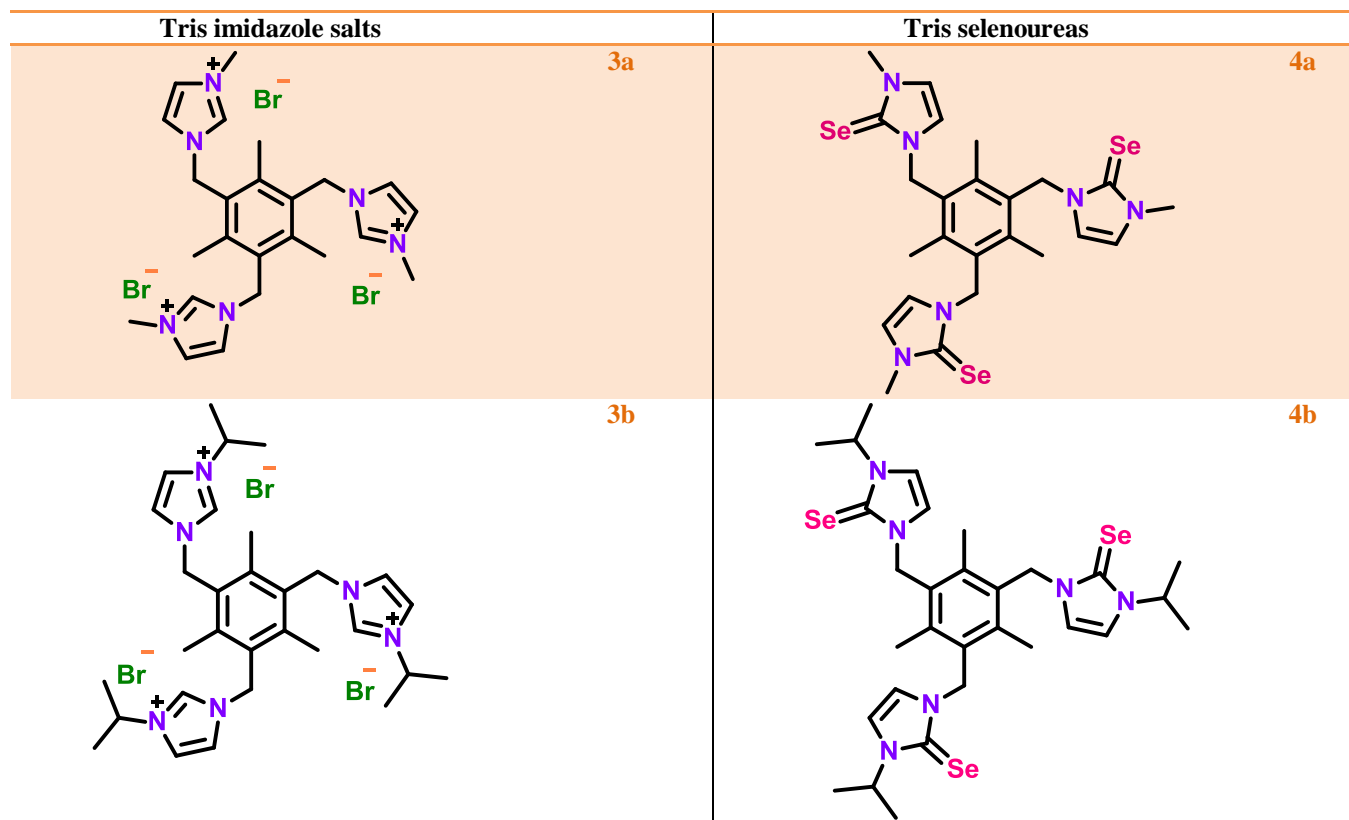
Selenium based antithyroid drugs exists in zwitterionic form where selenium carries the negative charge this leads to higher activity of selenium based drugs than that of sulfur based ^[8].

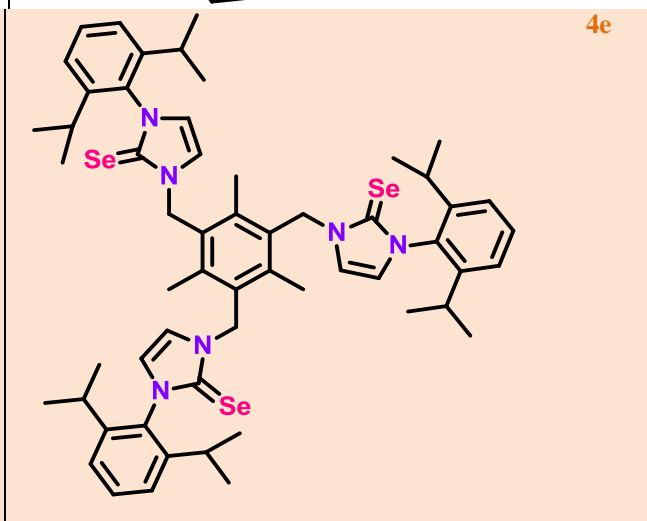
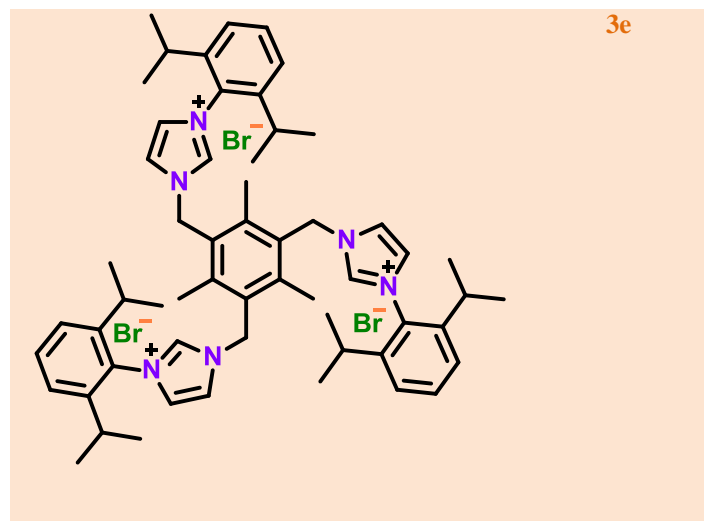
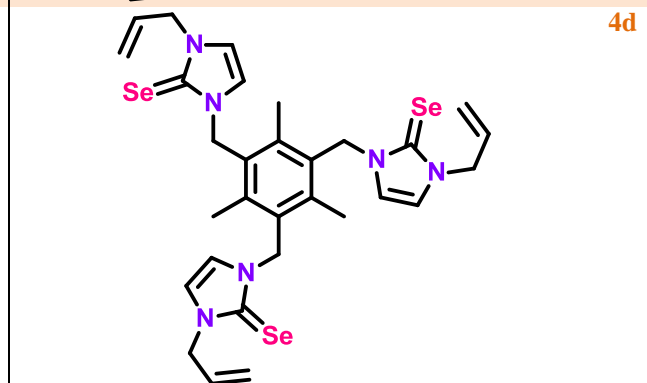
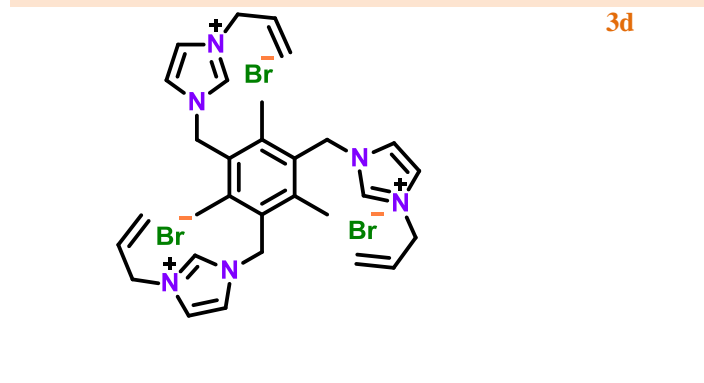
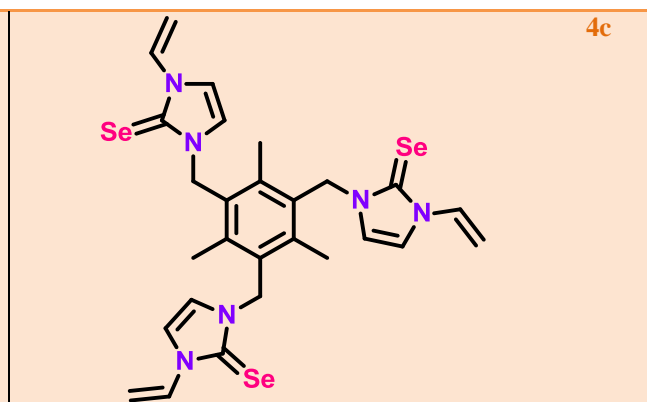
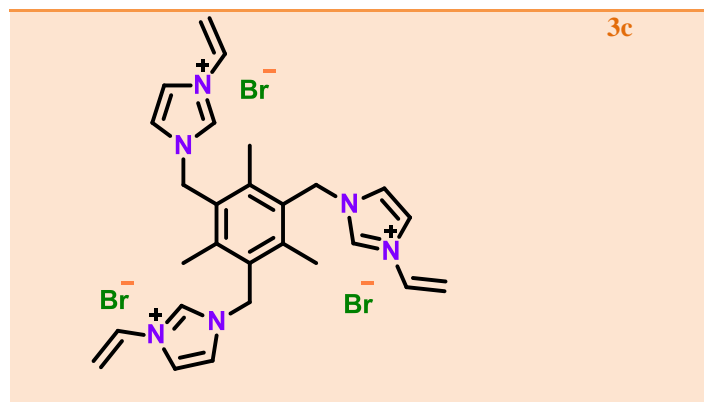
Recently it has been seen that if we incorporate more than one selenium in one molecule it's inhibition potency increases as an antithyroid drug ^[14].

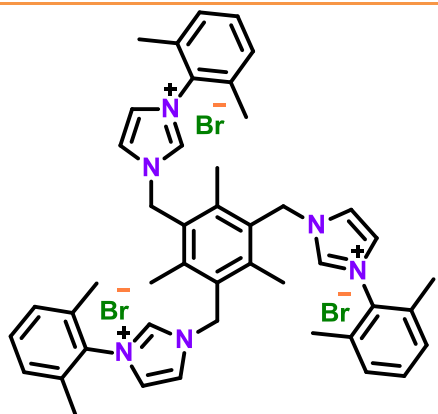
2. Aim of work

Our aim is to synthesize and structurally characterize the antithyroid drug analogues of tris selones.

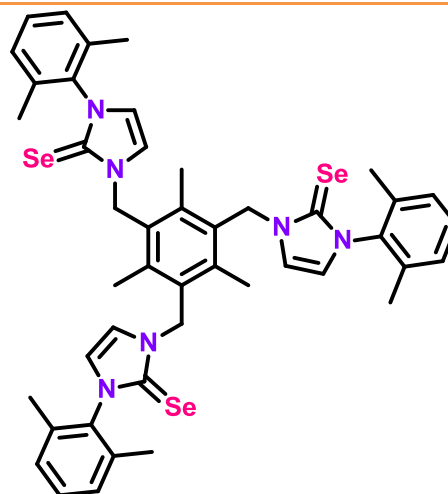
2.1. Target molecules







3f



4f

Figure 4. Chemical structures of tris imidazole salts and tris selones

3. Experimental section

3.1. General consideration

All manipulations were carried out under nitrogen using Schlenk vacuum line techniques. The solvents were purchased from commercial sources and purified according to standard procedures.^[15] [1,3,5-tris(bromomethyl)-2,4,6-trimethylbenzene mesityl tris methylene bromide] (**1**) was prepared as previously reported^[16], N-Substituted imidazoles were synthesized from reported procedures^[17]. Starting materials were purchased from commercial sources and used without further purification. FT-IR measurement (neat) was carried out on a Bruker Alpha-P Fourier transform spectrometer. The UV-vis spectra were measured on a T90+ UV-visible spectrophotometer. The fluorescent spectra were measured on a Fluoromax-4P TCSPC, Horiba Scientific spectrophotometer. High-resolution mass spectra (HR-MS) were recorded on an Agilent 6538 UHD Q-TOF. NMR spectra were recorded on Bruker Ultrashield-400 MHz spectrometers at 25 °C unless otherwise stated. Chemical shifts are given relative to Me₄Si and were referenced to the solvent resonances as internal standards. The crystal structures of **4a-4d** and were measured on an Oxford Xcalibur 2 diffractometer. Data were collected at 150 K (for **4a**, **4b**) and 298 K (for **4c**, and **4d**). The structure of **4a-4e** were solved by direct methods using the SIR-97 program^[18] and refined with a full matrix least-squares method on F2 using the SHELXL-97 program^[19,20]. CCDC 000000-000000 contains the supplementary crystallographic data for this paper. These data can be obtained free of charge from the Cambridge Crystallographic Data Centre via www.ccdc.cam.ac.uk/data_request/cif or from the Cambridge Crystallographic Data Centre, 12 Union Road, Cambridge CB2 1EZ, UK; fax: +44 1223 336 033; or e-mail: deposit@ccdc.cam.ac.uk.

3.2. Synthesis and characterization of 1,1',1''-((2,4,6-trimethylbenzene-1,3,5-triyl)tris(methylene))tris(3-alkyl/aryl-1H-imidazol-3-ium) bromide (**3**)

To a stirred solution of 1,3,5-tris(bromomethyl)-2,4,6-trimethylbenzene in acetonitrile, 1-alkyl/aryl imidazole (4 eq) was added under nitrogen atmosphere, then the reaction mixture was stirred at 90 °C for 3 days. The reaction progress was monitored by TLC. After 3days the precipitate formed in the reaction

mixture was filtered washed with diethylether then dried under high vacuum for 4 h to get desired compound in analytically pure-form.

3b. White solid. Yield 76% (based on **1**). M.P., 281-284 °C. FT-IR (neat, $\bar{\nu}$): 3393 (m), 3125 (w), 3059 (m), 2978 (m), 1625 (w), 1550 (m), 1456 (w), 1431 (w), 1377 (w), 1330 (w), 1299 (w), 1269 (w), 1177 (m), 1149 (s) cm^{-1} . ^1H NMR (CDCl_3 , 400 MHz): δ 10.10 (s, 3H, N-CH-N), 8.39 (s, 3H, Im-H), 7.31 (s, 3H, Im-H), 5.82 (s, 6H, Mes- CH_2 -Im), 5.05-4.98 (m, 3H, N- $\text{CH}(\text{CH}_3)_3$), 2.36 (s, 9H, Ar- CH_3), 1.53-1.52 (d, 18H, $J_{\text{HH}} = 6.4$ Hz, N- $\text{CH}(\text{CH}_3)_3$) ppm. ^{13}C NMR δ 140.96 (ArC), 134.62 (N-CH-N), 129.17 (ArC), 122.56 (Im-CH), 120.18 (Im-CH), 52.12 (N- $\text{CH}(\text{CH}_3)_3$), 47.75 (Mes- CH_2 -Im), 22.26 (N- $\text{CH}(\text{CH}_3)_3$), 16.26 (Ar- CH_3) ppm. HRMS (+ESI): calcd. for $\text{C}_{30}\text{H}_{45}\text{Br}_2\text{N}_6^+$ 647.2072; found 647.2076.

3c. Off white solid. Yield 88% (based on **1**). M.P., above 300 °C. FT-IR (neat, $\bar{\nu}$): 3381 (w), 3095 (w), 3070 (m), 3045 (m), 3002 (w), 2963 (m), 1647 (m), 1569 (m), 1545 (m), 1485 (w), 1335 (w), 1243 (w), 1220 (w), 1159 (s) cm^{-1} . ^1H NMR (D_2O , 400 MHz): δ 7.84-7.83 (d, 3H, $J_{\text{HH}} = 2.4$ Hz, Im-H), 7.48-7.47 (d, 3H, $J_{\text{HH}} = 2$ Hz, Im-H), 7.12-7.06 (q, 3H, N- CHCH_2), 5.81-5.76 (dd, 3H, $J_{\text{HH}} = 2.8$ Hz, N- CHCH_2), 5.64 (s, 6H, Mes- CH_2 -Im), 5.43-5.40 (dd, 3H, $J_{\text{HH}} = 2.8$ Hz, N- CHCH_2), 2.36 (s, 9H, Ar- CH_3) ppm. ^{13}C NMR ($\text{DMSO}-d_6$, 100 MHz): δ 141.66 (ArC), 135.13 (N-CH-N), 128.86 (ArC), 128.77 (N- CHCH_2), 123.49 (Im-CH), 118.75 (Im-CH), 108.31 (N- CHCH_2), 48.19 (Mes- CH_2 -Im), 16.47 (Ar- CH_3) ppm. HRMS (+ESI): calcd. for $\text{C}_{27}\text{H}_{33}\text{Br}_2\text{N}_6^+$ 599.1133; found 599.1134.

3d. White solid. Yield 65% (based on **1**). M.P., 135-137°C. FT-IR (neat, $\bar{\nu}$): 3399 (m), 3124 (w), 3077 (w), 3014 (m), 2972 (w), 2926 (w), 1643 (w), 1574 (w), 1554 (s), 1495 (w), 1443 (w), 1417 (m), 1384 (w), 1340 (w) cm^{-1} . ^1H NMR (D_2O , 400 MHz): δ 7.53-7.52 (d, 3H, $J_{\text{HH}} = 2$ Hz, Im-H), 7.43-7.42 (d, 3H, $J_{\text{HH}} = 2.4$ Hz, Im-H), 6.06-5.98 (m, 3H, N- CH_2CHCH_2), 5.61 (s, 6H, Mes- CH_2 -Im), 5.42-5.28 (dd, 6H, $J_{\text{HH}} = 10.4$ Hz, N- CH_2CHCH_2), 2.33 (s, 9H, Ar- CH_3) ppm. ^{13}C NMR (D_2O , 100 MHz): δ 141.62 (ArC), 130.46 (N- CH_2CHCH_2), 129.05 (ArC), 122.86 (Im-CH), 122.06 (Im-CH), 120.74 (N- CH_2CHCH_2), 51.62 (N- CH_2CHCH_2), 48.18 (Mes- CH_2 -Im), 15.74 (Ar- CH_3) ppm. HRMS (+ESI): calcd. for $\text{C}_{30}\text{H}_{39}\text{Br}_3\text{N}_6$ 720.0786; found 720.0805.

3e. Off white solid. Yield 79% (based on **1**). M.P., 241-243 °C. FT-IR (neat, $\bar{\nu}$): 3383 (w), 3111 (w), 3030 (w), 2961 (s), 2927 (m), 2868 (m), 2032 (w), 1623 (w), 1592 (w), 1540 (s), 1457 (s), 1418 (w),

1384 (w), 1364 (m) cm^{-1} . ^1H NMR (CDCl_3 , 400 MHz): δ 10.57 (s, 3H, N-CH-N), 8.89 (s, 3H, Im-H), 7.49-7.45 (t, 3H, ArH), 7.25-7.23 (d, 6H, $J_{HH} = 8\text{Hz}$, ArH), 7.06 (s, 3H, Im-H) 6.19 (s, 6H, Mes- CH_2 -Im), 2.50 (s, 9H, Ar- CH_3), 2.41-2.24 (m, 6H, Ar- $\text{CH}(\text{CH}_3)_2$), 1.20-1.10 (dd, 36H, $J_{HH} = 6.8\text{Hz}$ Ar- $\text{CH}(\text{CH}_3)_2$) ppm. ^{13}C NMR (CDCl_3 , 100 MHz): δ 144.99 (ArC), 142.28 (ArC), 137.55 (ArC), 131.59 (N-CH-N), 130.17 (ArC), 128.56 (ArC), 124.55 (ArC), 124.51 (Im-CH), 124.11 (Im-CH), 49.31 (Mes- CH_2 -Im), 28.65 (Ar- $\text{CH}(\text{CH}_3)_2$), 24.48 (Ar- $\text{CH}(\text{CH}_3)_2$), 24.40 (Ar- $\text{CH}(\text{CH}_3)_2$), 17.43 (Ar- CH_3) ppm.

3f. Off white solid. Yield 75% (based on **1**). M.P., 228-230 $^\circ\text{C}$. FT-IR (neat, $\bar{\nu}$): 3397 (m), 3112 (w), 2980 (w), 2922 (w), 2859 (w), 1622 (w), 1545 (s), 1474 (s), 1450 (m), 1384 (w), 1331 (w), 1181 (s), 1100 (s), 1062 (m) cm^{-1} . ^1H NMR (D_2O , 400 MHz): δ 7.74 (s, 3H, Im-H), 7.67 (s, 3H, Im-H), 7.44-7.40 (t, 3H, ArH), 7.29-7.27 (d, 6H, $J_{HH} = 7.6\text{Hz}$, ArH), 5.80 (s, 6H, Mes- CH_2 -Im), 2.46 (s, 9H, Ar- CH_3), 2.01 (s, 18H, Ar- CH_3) ppm. ^{13}C NMR (D_2O , 100 MHz): δ 141.77 (ArC), 134.72 (ArC), 133.13 (ArC), 130.86 (ArC), 129.37 (ArC), 128.78 (ArC), 124.57 (Im-CH), 122.98 (Im-CH), 48.71 (Mes- CH_2 -Im), 16.55 (Ar- CH_3), 15.94 (Ar- CH_3) ppm. HRMS (+ESI): calcd. for $\text{C}_{45}\text{H}_{51}\text{Br}_3\text{N}_6$ 912.1725; found 912.1722.

3.3. Synthesis and characterization of 3,3',3''-((2,4,6-trimethylbenzene-1,3,5-triyl)tris(methylene))tris(1-(2,6-alkyl/aryl)-1H-imidazole-2(3H)-selenone) (**4**)

An oven dried schlenk tube was equipped with 1,1',1''-((2,4,6-trimethylbenzene-1,3,5-triyl)tris(methylene))tris(3-alkyl/aryl-1H-imidazol-3-ium) bromide (1eq.), potassium carbonate (6eq.) and selenium powder (6eq.) under nitrogen atmosphere, subsequently MeOH was added then the reaction mixture was stirred for 36 h at 70 $^\circ\text{C}$. The reaction progress was monitored by TLC. After 36 h reaction mixture was filtered through celite, washed with DCM (4 X 5 mL) then the combined organics were evaporated to get white solid followed by workup with DCM (2 X 20 mL) and water (15 mL), gave analytically pure form of compound as white solid. The suitable crystals for X-ray analysis were grown in DCM/MeCN mixture (2:1) at 8 $^\circ\text{C}$.

4b. White solid. Yield 74% (based on **3**). M.P., 236-238 $^\circ\text{C}$. FT-IR (neat, $\bar{\nu}$): 3121 (w), 3082 (w), 2971 (w), 2924 (m), 2854 (w), 1561 (w), 1459 (w), 1425 (m), 1407 (s), 1366 (m), 1331 (m), 1293 (w), 1218 (m), 1196 (m) cm^{-1} . ^1H NMR (CDCl_3 , 400 MHz): δ 6.83-6.82 (d, 3H, $J_{HH} = 2.4\text{Hz}$, Im-H), 6.25-6.24 (d, 3H, $J_{HH} = 2.4\text{Hz}$, Im-H), 5.29 (s, 6H, Mes- CH_2 -Im), 5.25-5.22 (m, 3H, N-CH-(CH_3)₃), 2.18 (s, 9H, Ar- CH_3), 1.39-1.38 (d, 18H, $J_{HH} = 6.8\text{Hz}$, N-CH(CH_3)₃) ppm. ^{13}C NMR (CDCl_3 , 100 MHz): δ 154.65 (C=Se),

139.95 (ArC), 131.22 (ArC), 116.95 (Im-CH), 115.04 (Im-CH), 50.88 (N-CH(CH₃)₂), 48.64 (Mes-CH₂-Im), 21.92 (N-CH(CH₃)₂), 16.81 (Ar-CH₃) ppm.

4c. Brown solid. Yield 75% (based on **3**). M.P., 212-214 °C. FT-IR (neat, $\bar{\nu}$): 3161 (w), 3130 (w), 3086 (w), 2922 (w), 1692 (w), 1642 (s), 1564 (w), 1428 (s), 1325 (m), 1291 (w), 1225 (m), 1116 (w), 1042 (w) cm⁻¹. ¹H NMR (CDCl₃, 400 MHz): δ 7.69-7.63 (q, 3H, N-CHCH₂), 7.08-7.07 (d, 3H, J_{HH} = 2.4Hz, Im-*H*), 6.30-6.29 (d, 3H, J_{HH} = 4Hz, Im-*H*), 5.30 (s, 6H, Mes-CH₂-Im), 5.25-5.02 (dd, 6H, J_{HH} = 7.2Hz, N-CHCH₂), 2.23 (s, 9H, Ar-CH₃) ppm. ¹³C NMR (CDCl₃, 100 MHz): δ 157.53 (C=Se), 140.19 (ArC), 131.59 (N-CHCH₂), 131.02 (ArC) 117.69 (Im-CH), 114.96 (Im-CH), 102.45 (N-CHCH₂), 48.60 (Mes-CH₂-Im), 16.96 (Ar-CH₃) ppm.

4d. Off white solid. Yield 73% (based on **3**). M.P., 234-236 °C. FT-IR (neat, $\bar{\nu}$): 3129 (w), 3087(w), 2962 (w), 2917 (w), 1563 (w), 1440 (m), 1396 (s), 1327 (w), 1260 (m), 1235 (s), 1217 (s), 1178 (w), 1090 (m), 1016 (s). ¹H NMR (CDCl₃, 400 MHz): δ 6.79-6.78 (d, 3H, J_{HH} = 2.4 Hz, Im-*H*), 6.25-6.24 (d, 3H, J_{HH} = 2.4 Hz, Im-*H*), 5.97-5.90 (m, 3H, N-CH₂CHCH₂), 5.31 (s, 6H, Mes-CH₂-Im), 5.29-5.21 (m, 6H, N-CH₂CHCH₂), 4.80-4.78 (d, 6H, J_{HH} = 6.4 Hz, N-CH₂CHCH₂), 2.19 (s, 9H, Ar-CH₃) ppm. ¹³C NMR (CDCl₃, 100 MHz): δ 156.05 (C=Se), 139.98 (ArC), 131.42 (N-CH₂CHCH₂), 131.18 (ArC) 119.68 (N-CH₂CHCH₂), 118.56 (Im-CH), 116.73 (Im-CH), 51.93 (N-CH₂CHCH₂), 48.98 (Mes-CH₂-Im), 16.84 (Ar-CH₃) ppm.

4e. Off White solid. Yield 78% (based on **3**). M.P., 122-124 °C. FT-IR (neat, $\bar{\nu}$): 3162 (w), 3135 (w), 3073 (w), 2961 (m), 2924 (m), 2867 (m), 1560 (w), 1470 (m), 1416 (m), 1377 (m), 1349 (m), 1303 (w), 1260 (s), 1216 (m), 1088 (m), 1020 (s) cm⁻¹. ¹H NMR (CDCl₃, 400 MHz): δ 7.50-7.47 (t, 3H, Ar*H*), 7.31-7.29 (d, 6H, J_{HH} = 7.6Hz, Ar*H*), 6.83-6.82 (d, 3H, J_{HH} = 2Hz, Im-*H*), 6.50-6.49 (d, 3H, J_{HH} = 2.4Hz, Im-*H*), 5.50 (s, 6H, Mes-CH₂-Im), 2.50-2.47 (m, 6H, Ar-CH(CH₃)₂), 2.39 (s, 9H, Ar-CH₃) 1.33-1.32 (d, 18H, J_{HH} = 6.8Hz, Ar-CH(CH₃)₂), 1.11-1.09 (d, 18H, J_{HH} = 6.8Hz, Ar-CH(CH₃)₂) ppm. ¹³C NMR (CDCl₃, 100 MHz): δ 159.09 (C=Se), 146.09 (ArC), 139.87 (ArC), 133.83 (ArC), 131.91 (ArC), 130.34 (ArC), 124.25 (ArC), 121.18 (Im-CH), 116.96 (Im-CH), 49.27 (Mes-CH₂-Im), 29.65 (Ar-CH(CH₃)₂), 24.46 (Ar-CH(CH₃)₂), 23.33 (Ar-CH(CH₃)₂), 16.95 (Ar-CH₃) ppm.

4f. Off White solid. Yield 65% (based on **3**). M.P., 296-298 °C. FT-IR (neat, $\bar{\nu}$): 3149 (w), 3118 (w), 3077 (w), 2963 (w), 2917 (w), 2855 (w), 1727 (w), 1553 (w), 1478 (m), 1443 (w), 1416 (w), 1375 (s), 1332 (m), 1260 (w), 1120 (m) cm⁻¹. ¹H NMR (CDCl₃, 400 MHz): δ 7.32-7.28 (t, 3H, Ar*H*), 7.20-7.18 (d, 6H, J_{HH} = 7.6Hz, Ar*H*), 6.80-6.79 (d, 3H, J_{HH} = 2.4Hz, Im-*H*), 6.50-6.49 (d, 3H, J_{HH} = 2Hz, Im-*H*),

5.46 (s, 6H, Mes-CH₂-Im), 2.36 (s, 9H, Ar-CH₃), 2.07 (s, 18H, Ar-CH₃) ppm. ¹³C NMR (CDCl₃, 100 MHz): δ 156.84 (C=Se), 139.90 (ArC), 136.43 (ArC), 135.73 (ArC), 131.71 (ArC), 129.60 (ArC), 128.51 (ArC), 119.62 (Im-CH), 117.48 (Im-CH), 49.14 (Mes-CH₂-Im), 18.15 (Ar-CH₃), 16.96 (Ar-CH₃) ppm.

3.4. Preparation of solution of compounds for fluorescence spectroscopy

All the tris imidazole salts [1,1',1''-((2,4,6-trimethylbenzene-1,3,5-triyl)tris(methylene))tris(3-alkyl/aryl-1H-imidazol-3-ium) bromide] (**3**) (1.87×10^{-5} M) were dissolved in 25 mL DMSO. So that concentration of all the solutions was remain same.

Tris selones [3,3',3''-((2,4,6-trimethylbenzene-1,3,5-triyl)tris(methylene))tris(1-(2,6-alkyl/aryl)-1H-imidazole-2(3H)-selenone)] (**4**) were also dissolved in same concentration (1.87×10^{-5} M) in 25 mL DMSO keeping same concentration.

3.5. Preparation of solution of compounds for U.V-Vis spectroscopy

Solutions were prepared same as in the case of fluorescence for tris imidazole salts and tris selones.

3.6. Preparation of solutions for ¹H NMR study of compounds

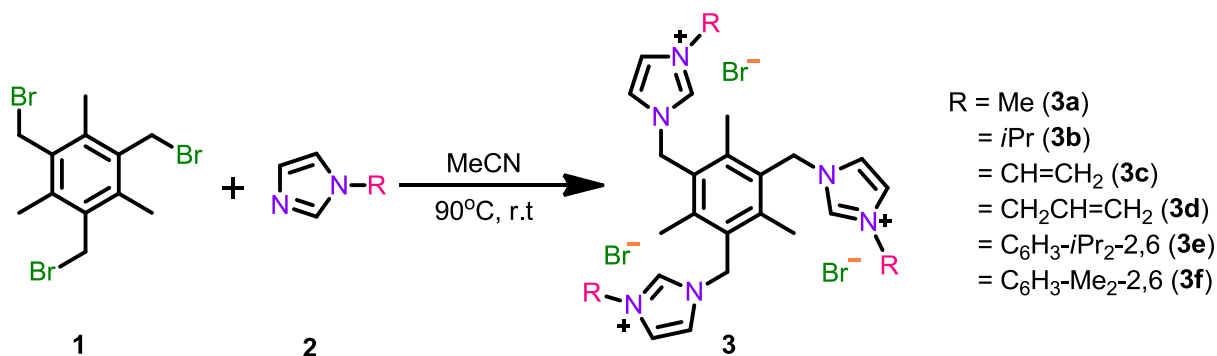
0.015g of each tris selones was taken in a thoroughly cleaned NMR tube and was dissolved in 0.5 mL of CDCl₃ at room temperature. For tris imidazole salts the amount of compound has taken for ¹H NMR is same but solvent varies for various compounds e.g D₂O has been used for compounds **3a**, **3c**, **3d**, **3f** and CDCl₃ for **3b**, **3e**.

3.7. Preparation of solutions for ¹³C NMR, DEPT, HSQC, HMBC study of compounds

0.025g of tris selone compounds have taken in a cleaned NMR tube and were dissolved in 0.5 mL of CDCl₃ at room temperature. Same amount of tris imidazole salts were taken but with various solvents. D₂O was used for **3a**, **3d**, **3f**, CDCl₃ for **3e** and DMSO-*d*₆ for **3b**, **3c**.

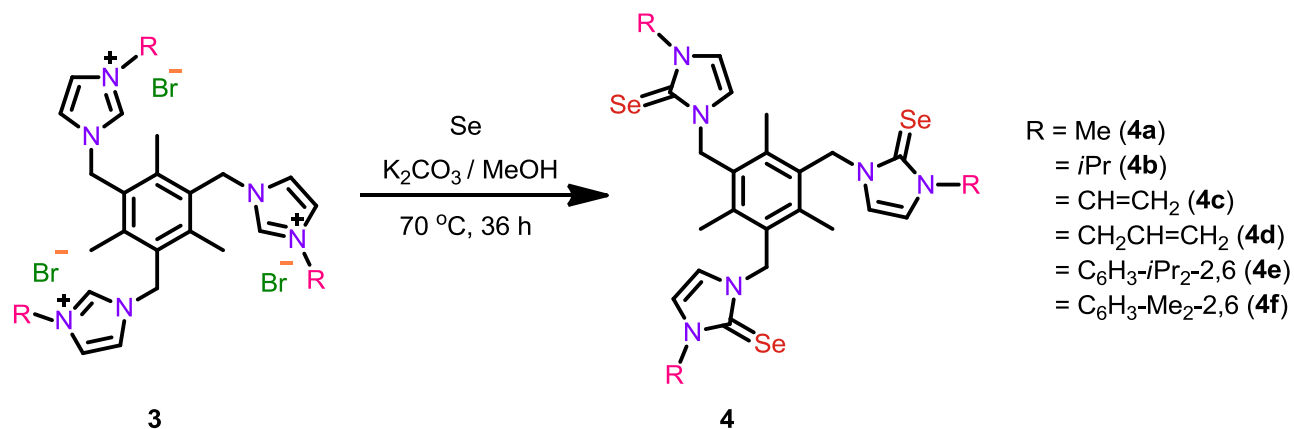
4. Scheme

4.1. Synthesis of 1,1',1''-((2,4,6-trimethylbenzene-1,3,5-triyl)tris(methylene))tris(3-alkyl/aryl-1H-imidazol-3-ium) bromide (3)



Scheme 2. Synthesis of 3a-3f

4.2. Synthesis of 3,3',3''-((2,4,6-trimethylbenzene-1,3,5-triyl)tris(methylene))tris(1-(2,6-alkyl/aryl)-1H-imidazole-2(3H)-selenone) (4)

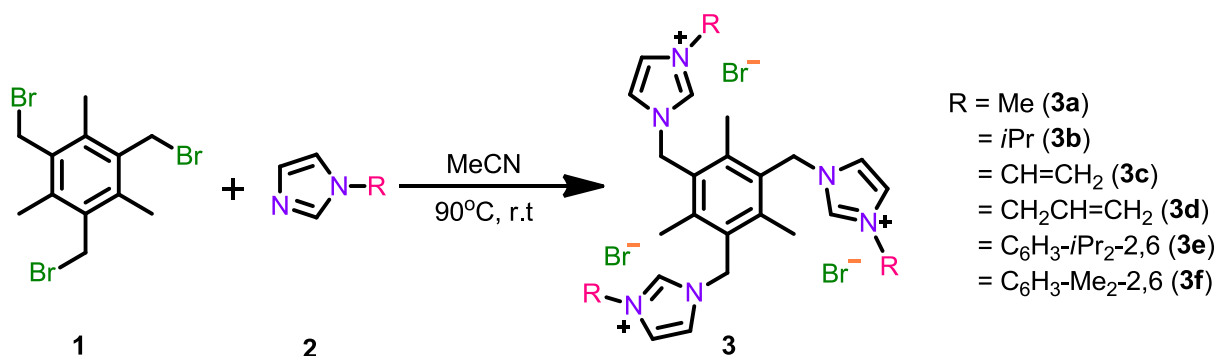


Scheme 3. Synthesis of 4a-4f

5. Results and discussion

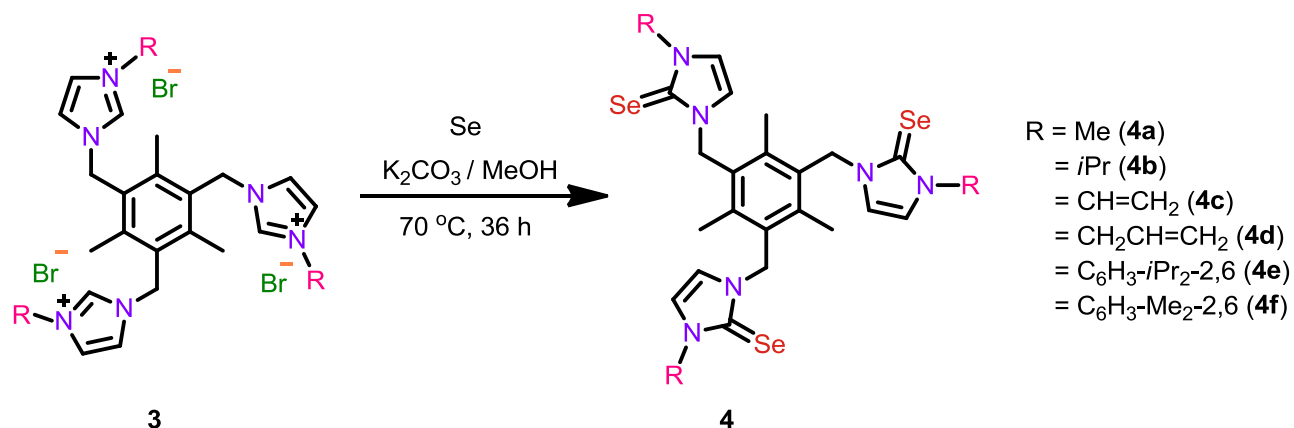
5.1. Synthesis and characterization of (3)

Compounds **3a-3f** were synthesized from the reaction between 1,3,5-tris(bromomethyl)-2,4,6-trimethylbenzene and 4 equivalence of N-substituted imidazole in acetonitrile at 90 °C for three days afford a large precipitate, which was purified by washing with diethyl ether or acetone to get analytical pure compounds with 65%, 76%, 88%, 65%, 79%, 75% yields respectively. And the product formation was confirmed by NMR (^1H , ^{13}C and DEPT) and further these were characterized by IR and Uv-visible technique. **3b-3f** were stable solids at normal atmosphere. **3a** is hygroscopic white solid.



5.2. Synthesis and characterization of (4)

Compounds **4a-4f** were synthesized from the reaction between **3a-3f**, 6 equivalence potassium carbonate and 6 equivalence of Se in methanol at 70 °C for two days afford a large precipitate, which was purified by washing with methanol to get analytical pure compounds with 60%, 74%, 75%, 73%, 78%, 65% yields respectively. And the product formation was confirmed by NMR (^1H , ^{13}C and DEPT) and further these were characterized by IR and Uv-visible technique. **4a-4f** were stable solids at normal atmosphere.



Scheme 3. Synthesis of 4a-4f

5.3. FT-IR Studies

The IR spectra exhibit intense N–C–N and C=Se stretching at about a range 1540-1554, 1110-1200 cm^{-1} for **3a-3f** and **4a-4f** respectively.

5.4. NMR Studies

The NMR spectra for the salts and selones were recorded in different deuterated solvents { CDCl_3 (**3b**, **3e**, **4a-4f**), D_2O (**3a**, **3c**, **3d**, **3f**)}, at room temperature. ^1H and ^{13}C chemical shifts were made on the basis of 2D (HSQC and HMBC) NMR experiments. Due to the low solubility of **3b**, **3c** in organic solvents, their ^{13}C NMR spectra were recorded in $\text{DMSO}-d_6$. ^1H NMR for selones in CDCl_3 spectrum exhibits in the aliphatic region singlet resonances for $\text{Ar}-\text{CH}_3$ (2.12-2.39 ppm) and $\text{Mes}-\text{CH}_2-\text{Im}$ (5.17-5.50 ppm) groups (**Figure 6**). For the corresponding salts the resonances are found in the following ranges: 2.33-2.50 ppm for $\text{Ar}-\text{CH}_3$ and 5.59-6.19 ppm for $\text{Mes}-\text{CH}_2-\text{Im}$ (**Figure 5**) For compounds **3b** and **3e** in CDCl_3 , ^1H NMR signals are downfield shifted δ 10.10, 10.57 ppm for N-CH-N proton whereas in compounds **4a-4f** this downfield proton's peak disappears. N-CH-N proton for Compounds **3a**, **3c**, **3d**, **3f** in D_2O also did not give any peak due to D_2O exchange. The –CH–CH– protons of the imidazole rings appear in the range 6.24-7.30, 7.06-8.89 ppm in the salts and in the selones, a downfield shift is observed. ^{13}C NMR spectrum of **3a-3f** and **4a-4f** exhibits the following pattern ranges of the values 15.74-17.43 and 16.81-16.96 ppm for $\text{Ar}-\text{CH}_3$ and 47.75-49.31, 48.60-49.27 ppm for $\text{Mes}-\text{CH}_2-\text{Im}$ respectively. In ^{13}C NMR the N-CH-N carbons of **3a-3f** are in a range of δ 131.59-134.62 ppm

(Figure 7) and Compounds **4a-4f** show a singlet in a range of δ 154.65-159.09 ppm (Figure 8) which prove the existence of C=Se group ^[21]. Compounds **3d** and **3f** did not show any peak in ¹³C NMR.

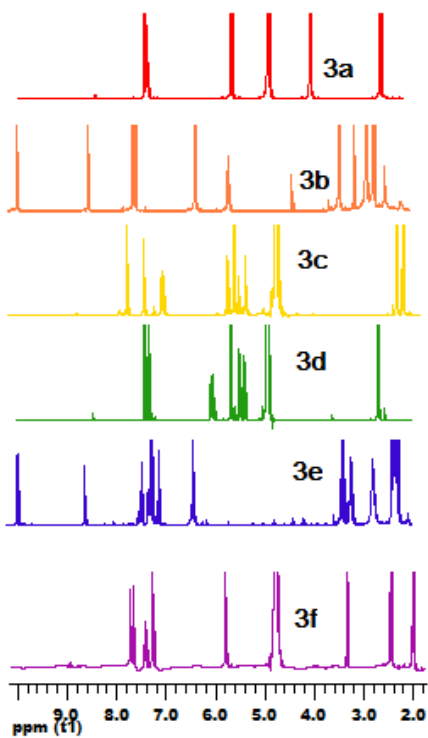


Figure 5. ¹H NMR spectra of **3a-3f** at RT.

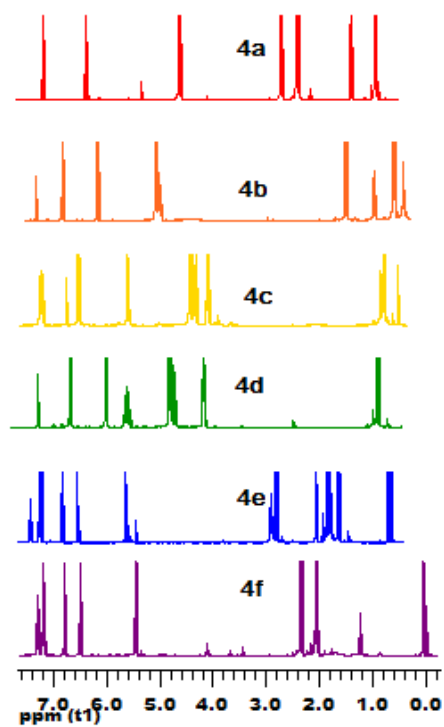


Figure 6. ¹H NMR spectra of **4a-4f** at RT.

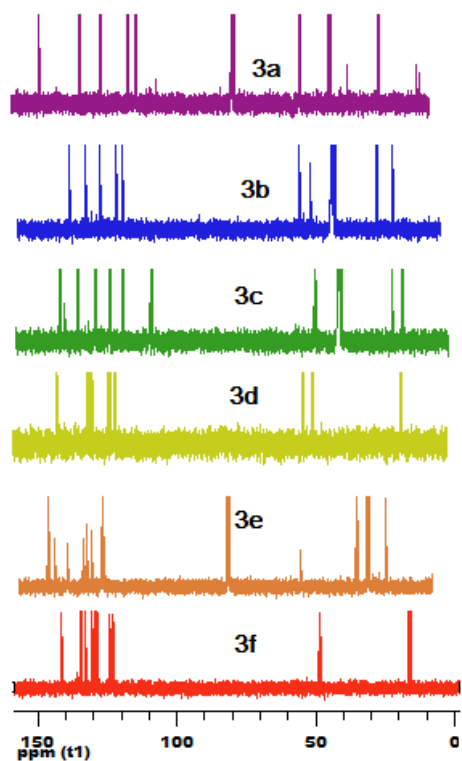


Figure 7. ^{13}C NMR spectra of **3a-3f** at RT.

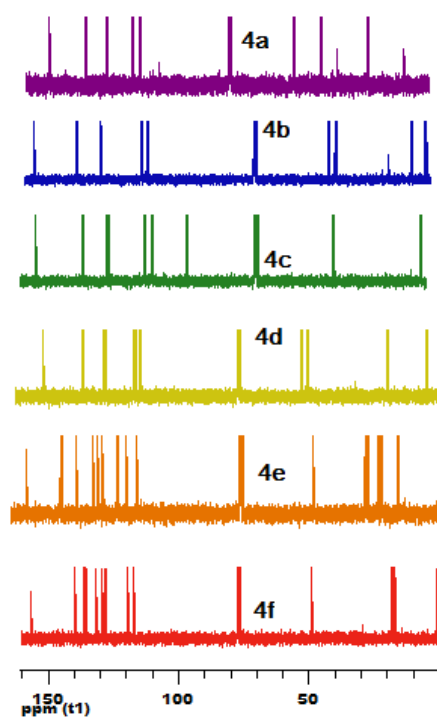


Figure 8. ^{13}C NMR spectra of **4a-4f** at RT.

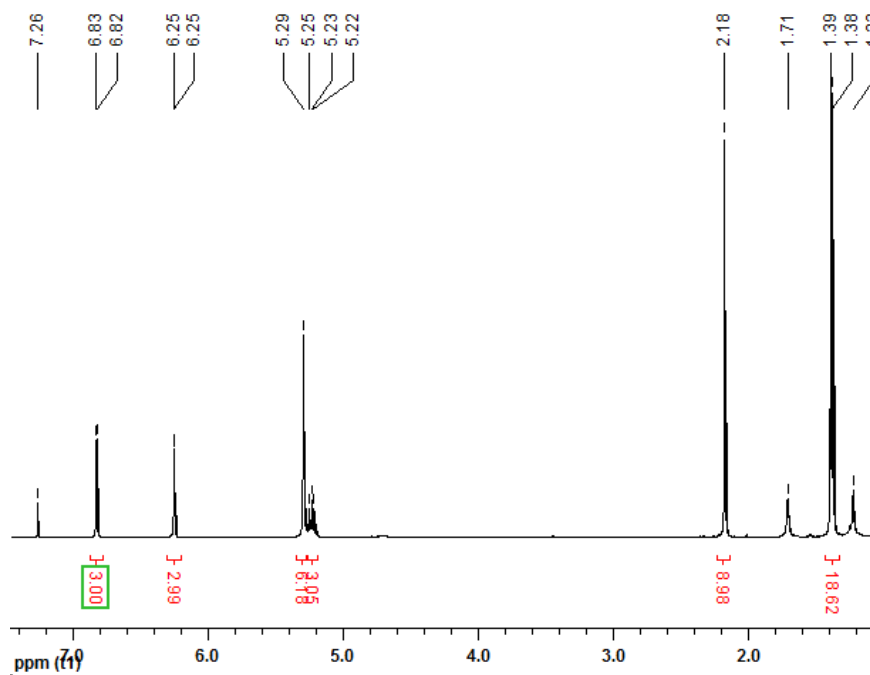


Figure 9. ^1H NMR spectrum (400 MHz, CDCl_3 , RT) of **4b**.

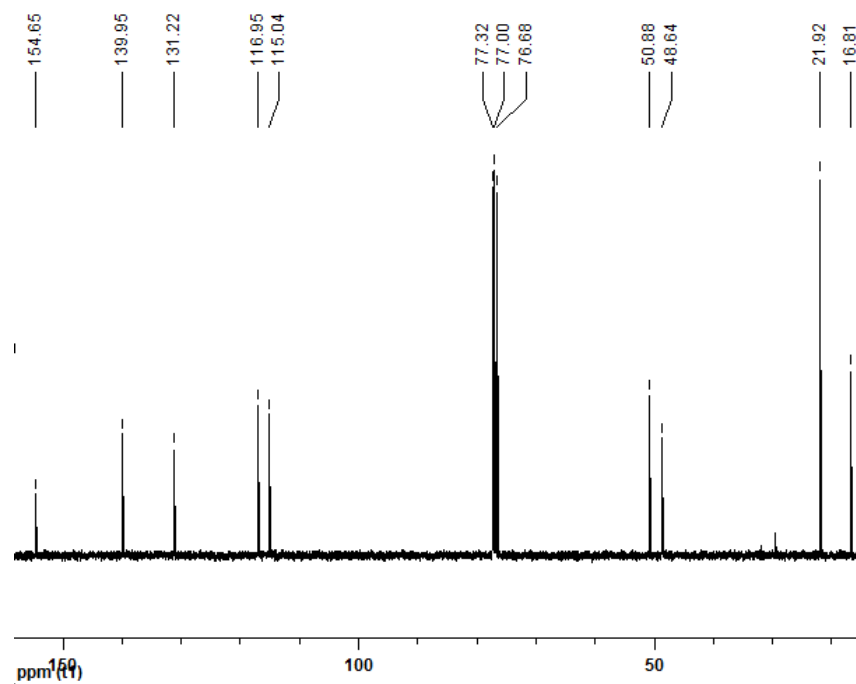


Figure 10. ^{13}C NMR spectrum (400 MHz, CDCl_3 , RT) of **4b**.

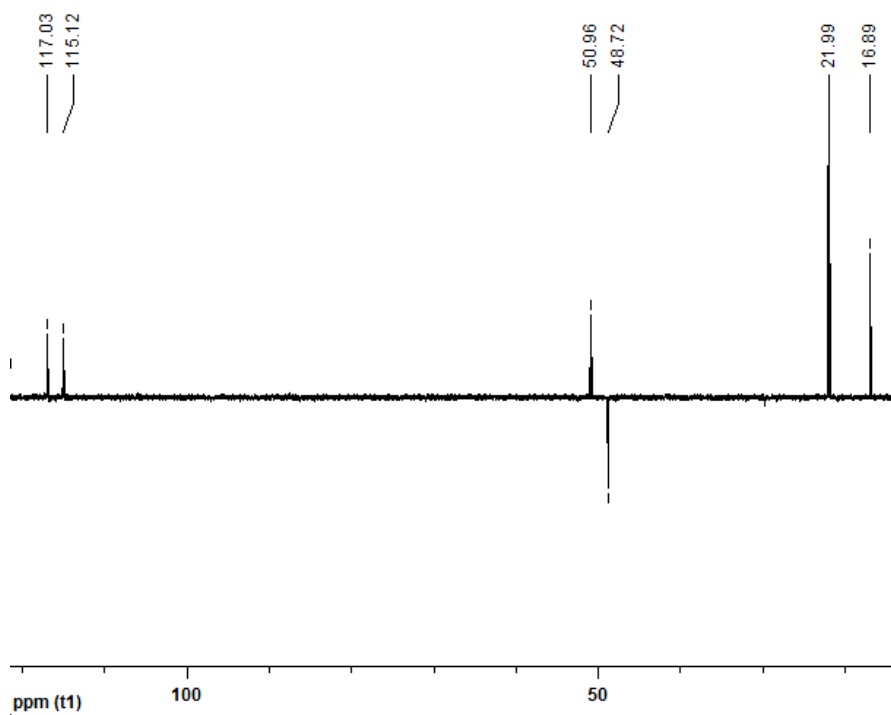


Figure 11. DEPT spectrum (400 MHz, CDCl_3 , RT) of **4b**.

2D NMR Spectrums

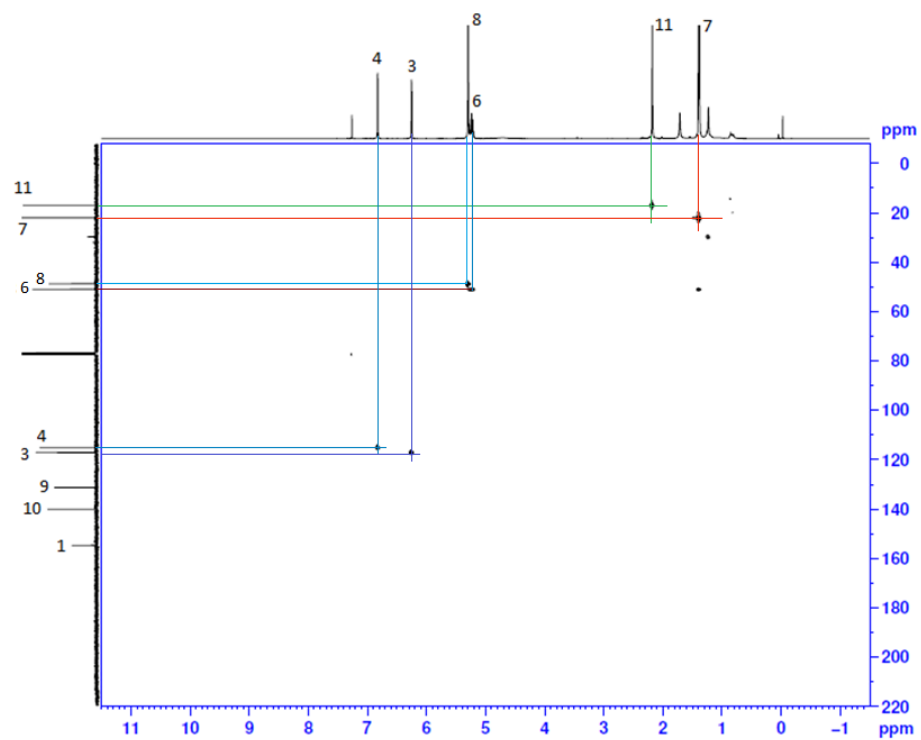


Figure 12. HSQC (400 MHz, CDCl₃, RT) of **4b**.

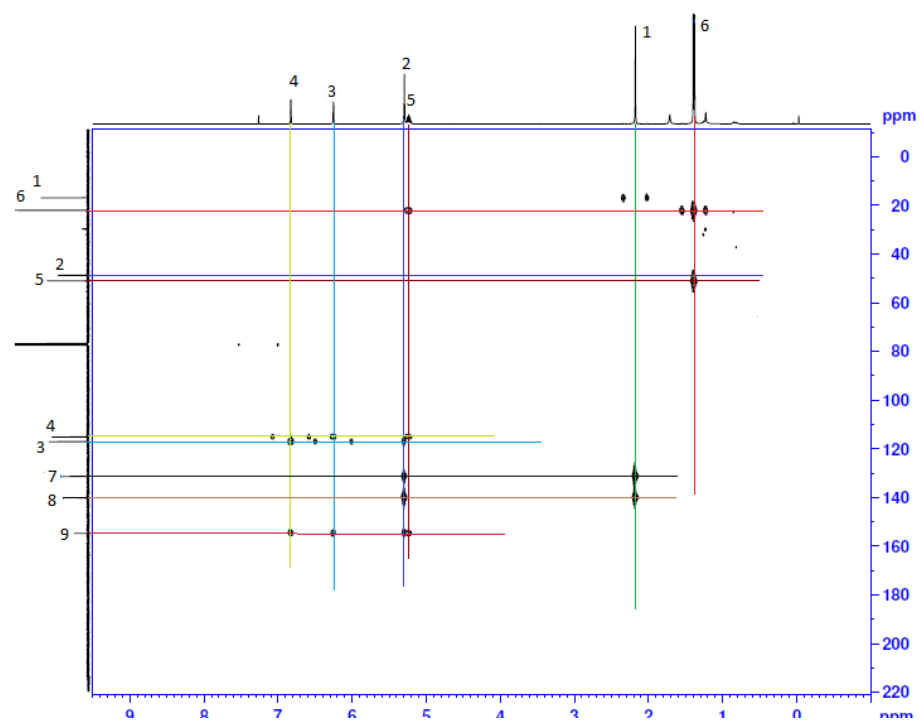


Figure 13. HMBC (400 MHz, CDCl₃, RT) of **4b**.

5.5. U-vis Studies

In order to understand electronic-structure property relationships for **4a-4f**, solution phase study ultraviolet–visible excitation were performed in DMSO at room temperature with concentration 1.87×10^{-5} M displayed a nearly comparable absorption maxima pattern at 258, 259, 279, 281, 284, 286 nm with an absorbance maxima value 0.5106 to 0.6443. Absorbance studies on the tris selone series are compiled graphically in (**Figure 14**), and selected optical properties are also shown in (**Table 1**). Compounds 4b-4f produce two absorption peaks one is sharp and other is comparably broad, are in a range of 257-259 nm and 279-314 nm, distinct absorptions due to $\pi-\pi^*$ transitions from their structural contributions. The π to π^* transition intensity is decreased in the order of **4f**, **4a**, **4b**, **4d**, **4e**, **4c**.

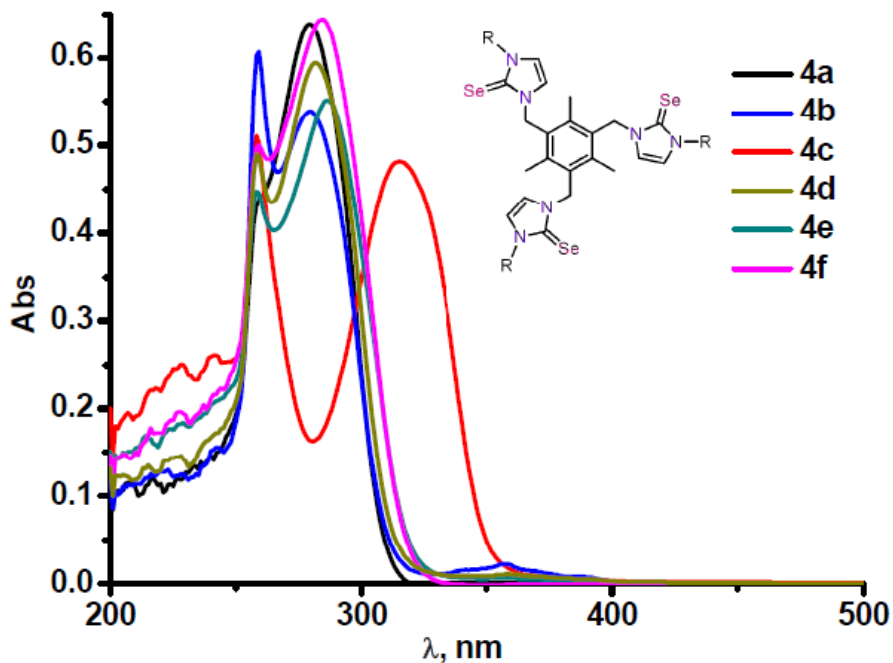


Figure 14. Solution absorbance spectra of compounds **4a-4f** (1.87×10^{-5} M) in DMSO

Entry	4a	4b	4c	4d	4e	4f
λ_{max} (nm)	279	259	258	281	286	284
$\log(\epsilon)^a$	4.5324	4.5099	4.4362	4.5008	4.4711	4.5372
Abs.	0.6372	0.6050	0.5106	0.5925	0.5533	0.6443

Table-1. ^a. ϵ reported in $\text{L mol}^{-1} \text{cm}^{-1}$

5.6. Crystal Structures

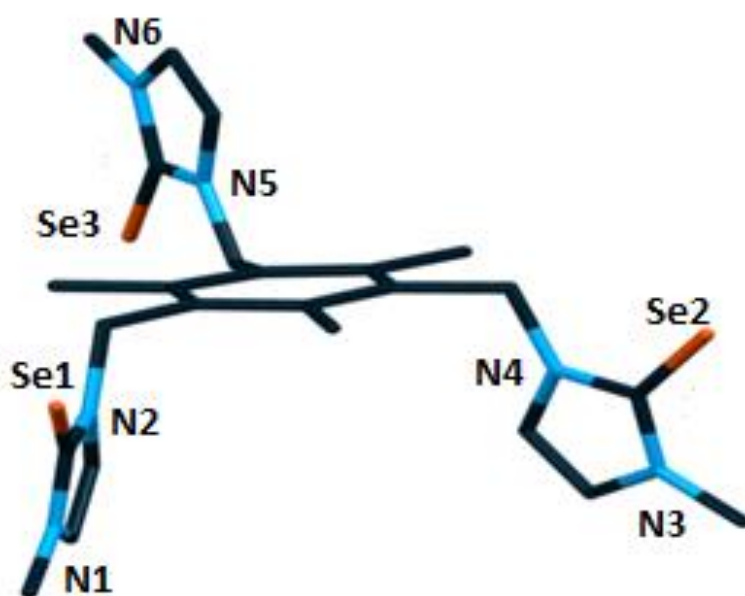


Figure 15. Structure of the asymmetric unit of **4a**.

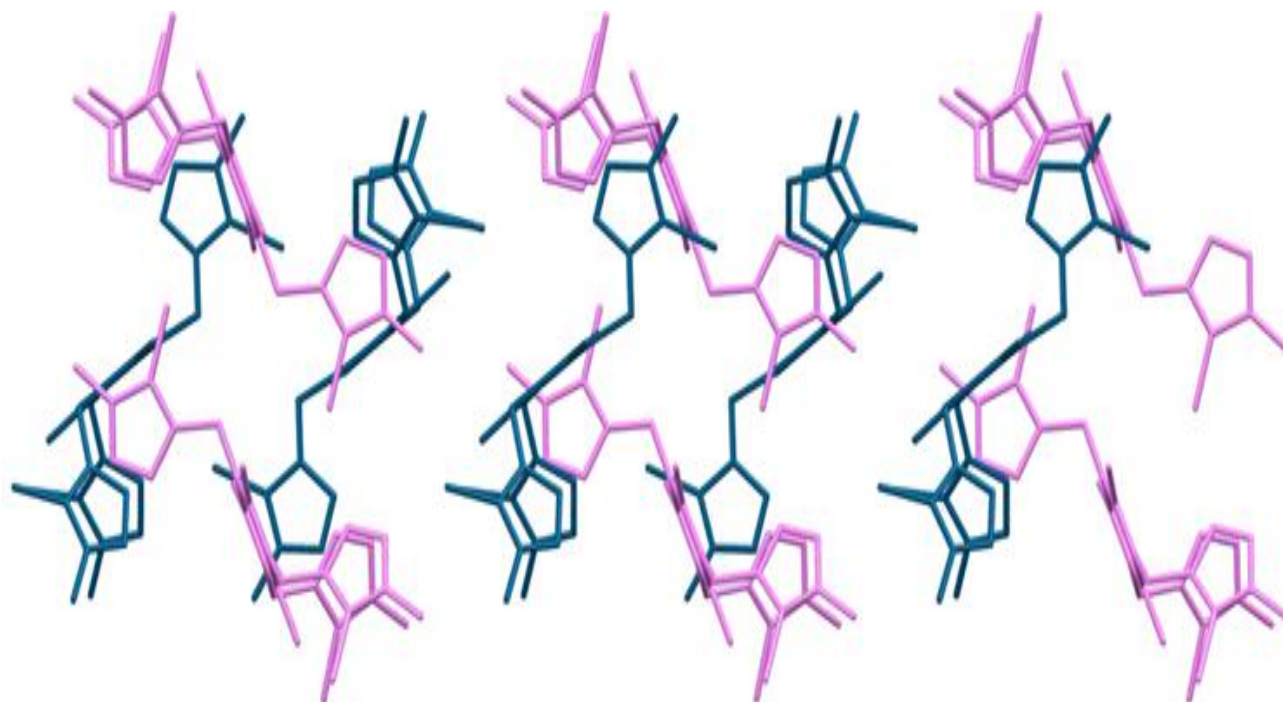


Figure 16. Molecular packing orientation of **4a** (View along c axis).

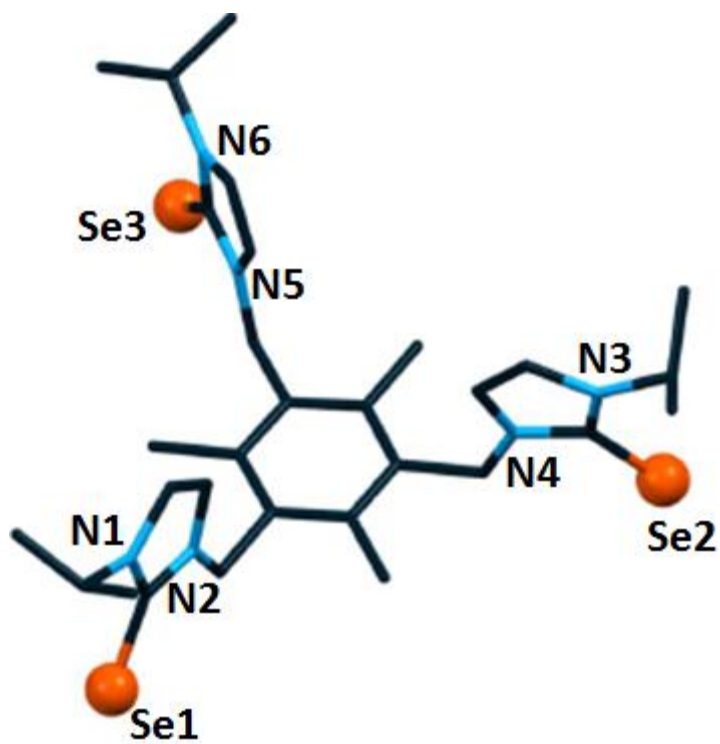


Figure 17. Structure of the asymmetric unit of **4b**.

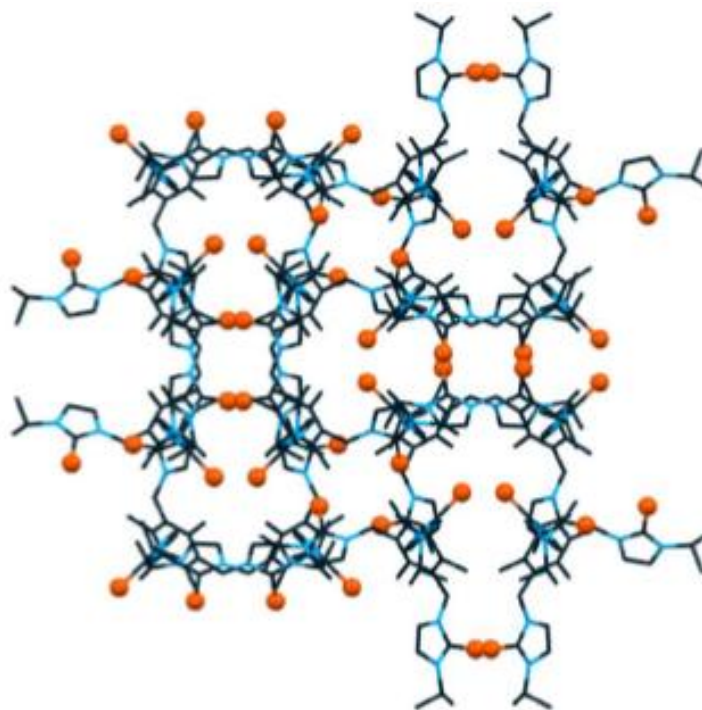


Figure 18. Molecular packing orientation of **4b** (View along b axis).

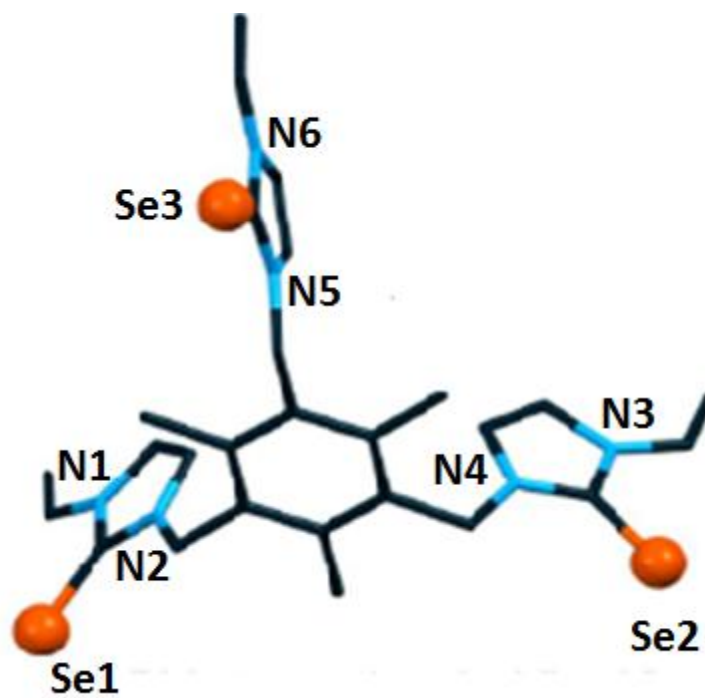


Figure 19. Structure of the asymmetric unit of **4c**.

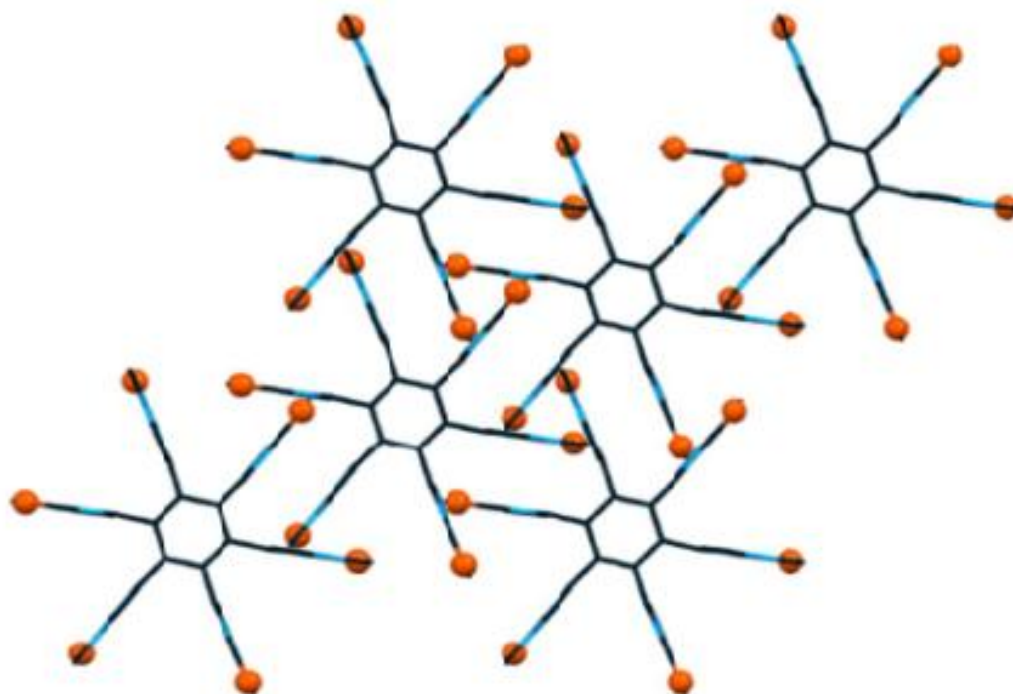


Figure 20. Molecular packing orientation of **4c** (View along c axis).

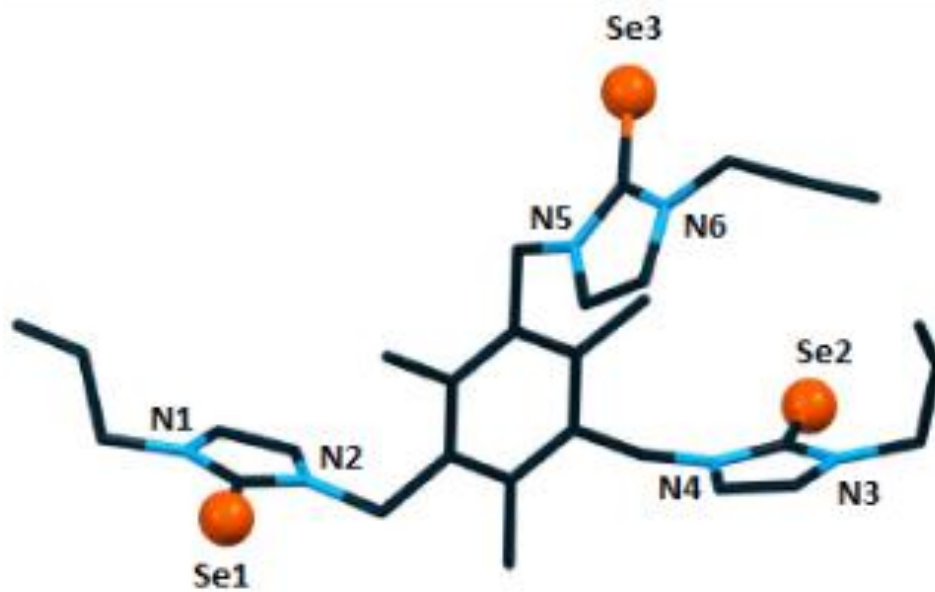


Figure 21. Structure of the asymmetric unit of **4d**.

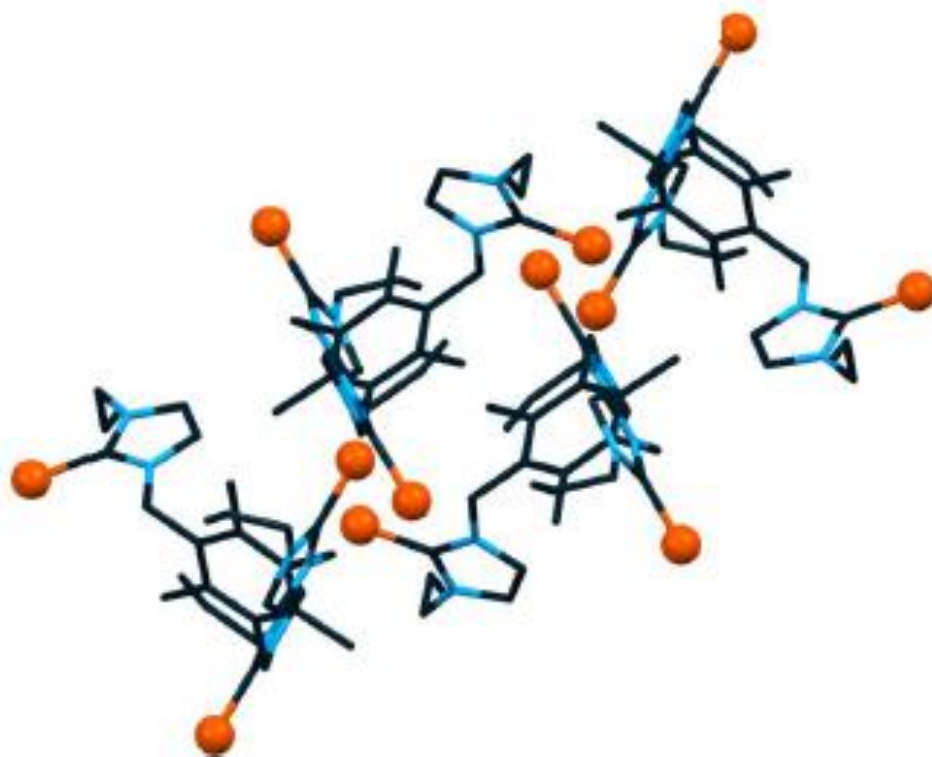


Figure 22. Molecular packing orientation of **4d** (View along c axis).

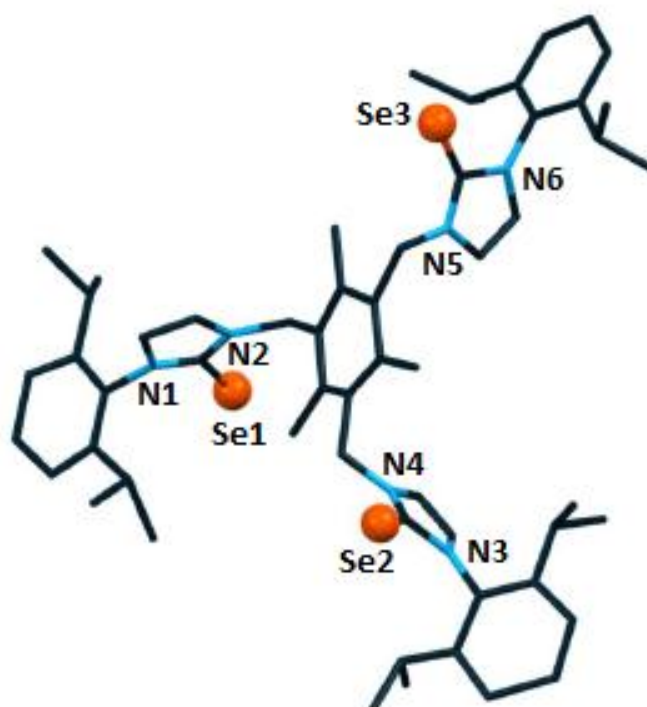


Figure 23. Structure of the asymmetric unit of **4e**.

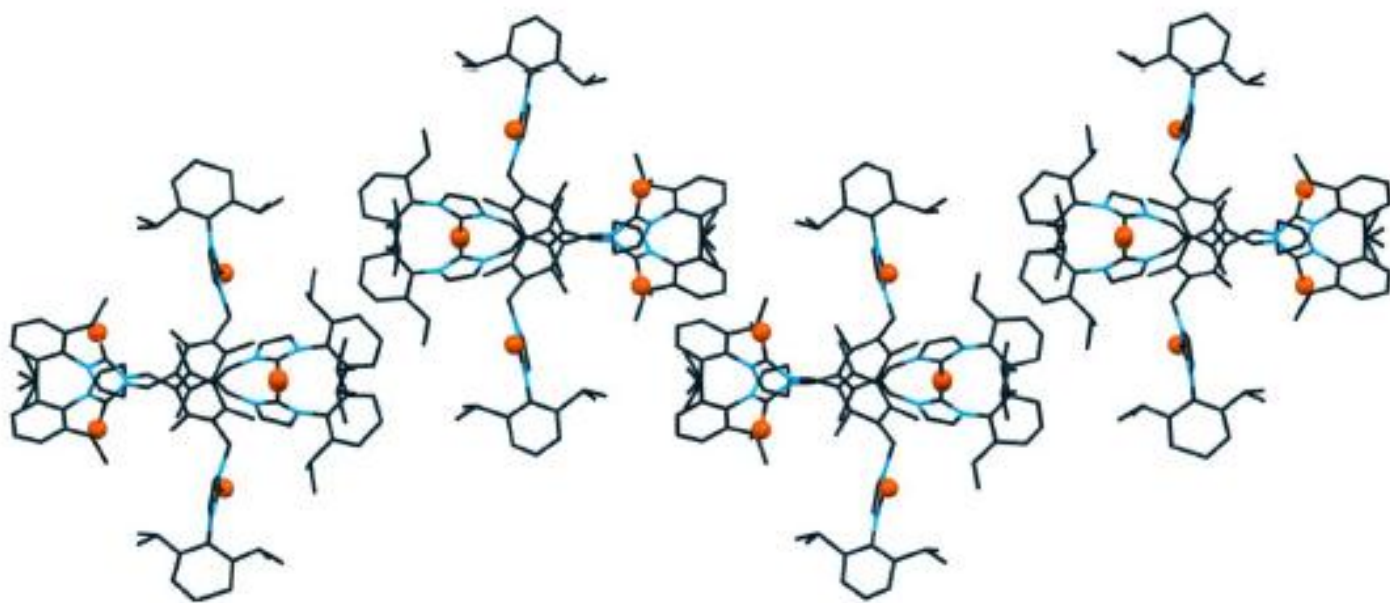


Figure 24. Molecular packing orientation of **4e** (View along c axis).

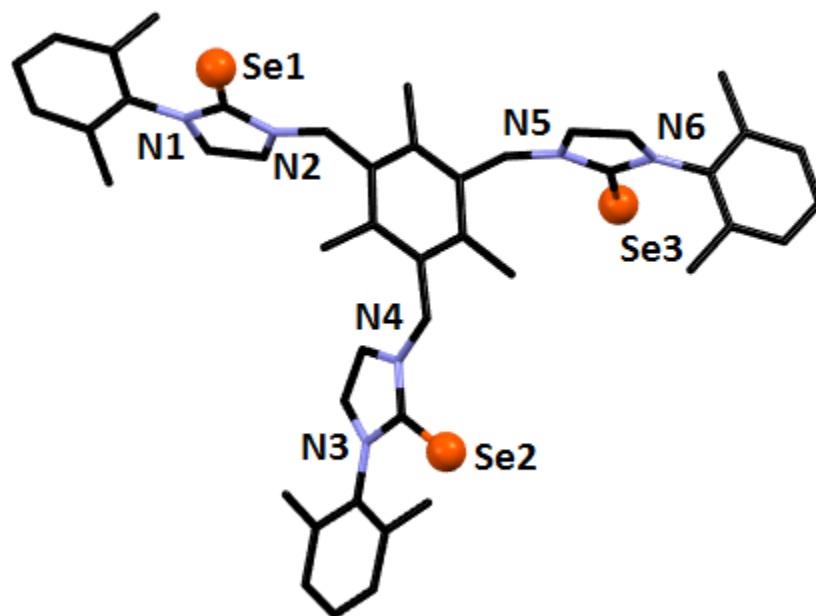


Figure 25. Structure of the asymmetric unit of **4f**.

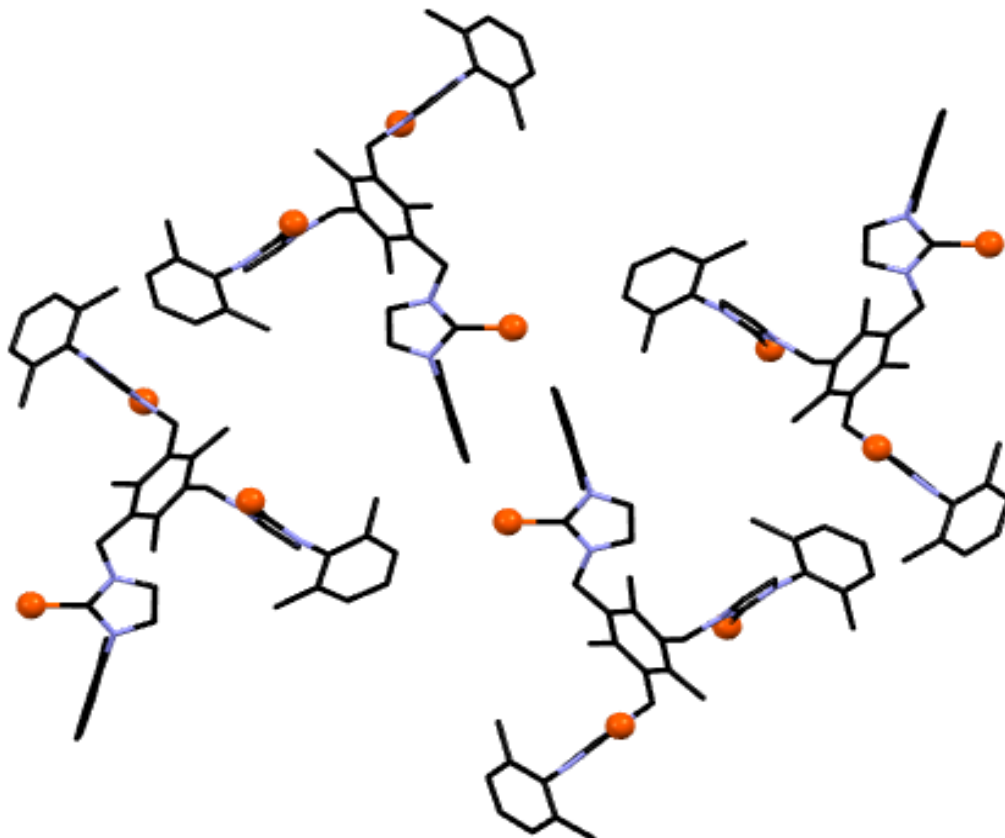


Figure 26. Molecular packing orientation of **4f** (View along a axis).

The crystal structure of the tris selenone and the complexes **4a**, **4b**, **4c**, **4d** and **4e** have been determined by single-crystal X-ray diffraction studies and selected bond lengths are presented in Tables 2 and 3 respectively.

The two imidazoline-2-selone in compounds **4a** are oriented in below and another one is in the above (**Figure 15**). Compound **4b** has the same selenourea moiety orientation as in compound **4a** i.e. two moieties are in downward and other is in upward (**Figure 17**). In compound **4c** all the selenourea moieties are aligned in the same upward direction (**Figure 19**). Next compound **4d** also has two selone group in below and third one in above (**Figure 21**). In case of compound **4e** two imidazole rings are facing in one side and another in opposite side (**Figure 23**). Compound **4f** got two selone group in the above of the plane of mesitylene and other one is in below (**Figure 25**).

To understand the nature of C–Se bonds in these selone derivatives, bond lengths of C–S/C–Se has to be compared with that of the previously reported thiourea compounds and our present compounds. Based on X-ray diffraction studies, average bond length of C–S is 1.683 Å which is quite shorter than the C–S single bond (1.810 Å) and slightly longer than the C–S double bond (1.610 Å)^[22] whereas the C–Se bond lengths in the tris selone compounds **4a** (1.844 Å), **4b** (1.850 Å), **4c** (1.827 Å), **4d** (1.827 Å) and **4e** (1.821 Å), **4f** (1.832 Å) (**Table-2**) are nearly comparable to the true C–Se single bond (1.940 Å). So we can conclude that the C–S bond in thione has more of double bond character than C–Se in selone, thus selones exist in its zwitterionic form where carbon has positive and selenium has a negative charge. The negative charge on selenium increases its nucleophilic activity^[23].

Compounds	Se–C (Å)	Avg. N–C (Å)	Angle ^o N–C–N
4a	1.844	1.354	104.9
4b	1.850	1.339	107.16
4c	1.827	1.362	105.79
4d	1.827	1.353	105.79
4e	1.821	2.058	104.23
4f	1.832	1.374	105.44

Table-2. Selected bond lengths and angles of **4a**, **4b**, **4c**, **4d**, **4e** and **4f**.

6. Conclusion

Since, the di-selenourea can inhibit PN-mediated nitration of BSA much actively than that of the mono-selenoureas, we have incorporated the three active selenium sites in a molecule. Thus, we have successfully synthesized a series of mesityl tris selone compounds **4a-4f** in highly pure form. The yield of **4a-4f** were excellent. Compounds **4a-4f** are stable toward moisture and air. The formation of **4a-4f** were confirmed by multinuclear 1D and 2D NMR studies like ¹H NMR, ¹³C NMR, DEPT, HSQC, HMBC. These new molecules were further studied by FT-IR and UV-vis spectroscopies. For the first time, the solid state structures of tris selone compounds, **4a-4f** were further confirmed by single crystal X-ray technique.

7. Reference

- [1] W. G. Jia, Y. B. Huang, Y. J. Lin, G. L. Wang and G. X. Jin, *Eur. J. Inorg. Chem.*, 2008, 4063-4073.
- [2] W. G. Jia, Y. B. Huang, Y. J. Lin and G. X. Jin, *Dalton Trans.*, 2008, 5612-5620.
- [3] D. Manna, G. Roy and G. Mugesh, *Acc. Chem. Res.*, 2013, **46** (11), 2706-2715.
- [4] (a) D. Behne, A. Kyriakopoulos, H. Meinhold and J. Ko^ohrle *Biochem. Biophys. Res. Commun.*, 1990, **173**, 1143-1149; (b) M. J. Berry, L. Banu and P. R. Larsen, *Nature*, 1991, **349**, 438-440; (c) M. J. Berry, J. D. Kieffer, J. W. Harney and P. R. Larsen, *J. Biol. Chem.*, 1991, **266**, 14155-14158; (d) J. Ko^ohrle, *Exp. Clin. Endocrinol.*, 1994, **102**, 63-89; (e) P. R. Larsen and M. J. Berry, *Annu. Rev. Nutr.*, 1995, **15**, 323-352; (f) St. Germain, D. L. and V. A. Galton, *Thyroid*, 1997, **7**, 655-668; (g) J. Ko^ohrle, *Biochimie*, 1999, **81**, 527-553; (h) W. W. du Mont, G. Mugesh, C. Wismach and P. G. Jones, *Angew. Chem.*, 2001, **40**, 2486-2489; (i) A. C. Bianco, D. Salvatore, B. Gereben, M. J. Berry and P. R. Larsen, *Endocr. Rev.*, 2002, **23**, 38-89; (j) J. Ko^ohrle, *Methods Enzymol.*, 2002, **347**, 125-167.
- [5] G. Roy and G. Mugesh, *J. Am. Chem. Soc.*, 2005, **127**, 15207-15217.
- [6] D. Manna, G. Roy and G. Mugesh, *Acc. Chem. Res.*, 2013, **46** (11), 2706-2715.
- [7] (a) J. Buxeraud, A. C. Absil, J. Claude, C. Raby, G. Catanzano and C. Beck, *Eur. J. Med. Chem.*, 1985, **20**, 43; (b) C. Raby, J. F. Lagorce, A. C. Jambut, J. Buxeraud and G. Catanzano, *Endocrinology*, 1990, **20**, 1683.
- [8] R. Bassosi, N. Niccolai and C. Rossi, *Biophys. Chem.*, 1978, **8**, 61-69.
- [9] D. Manna, G. Roy and G. Mugesh, *Acc. Chem. Res.*, 2013, **46** (11), 2706-2715.
- [10] K. P. Bhabak and G. Mugesh, *Inorganica Chimica Acta*, 2010, **363**, 2812-2818.
- [11] (a) G. Roy, D. Das and G. Mugesh, *Inorganica Chimica Acta*, 2007, **360**, 303-316; (b) K. P. Bhabak, K. Satheeshkumar, S. Jayavelu and G. Mugesh, *Org. Biomol. Chem.*, 2011, **9**, 7343; (c) F. Cristiani, F. A. Devillanova, A. Diaz and G. Verani, *Phosphorus and Sulfur and the Related Elements*, 1984, **20**(2), 231-240.
- [12] (a) W. G. Jia, Y. B. Huang, Y. J. Lin and G. X. Jin, *Dalton Trans.*, 2008, 5612-5620; (b) A. Huffer, B. Jeffery, B. J. Waller and A. A. Danopoulos, *C. R. Chimie*, 2013, **16**, 557-565.
- [13] K. P. Bhabak and G. Mugesh, *Inorganica Chimica Acta*, 2010, **363**, 2812-2818.
- [14] K. P. Bhabak, K. Satheeshkumar, S. Jayavelu and G. Mugesh, *Org. Biomol. Chem.*, 2011, **9**, 7343.

- [15] D. D. Perrin and W. L. F. Armarego, *Purification of laboratory chemicals*, London, 3rd edn, 1988.
- [16] A. W. van der Made and R.H. van der Made, *J. Org. Chem.*, 1993, **58**, 1262-1263.
- [17] O.V. Starikova, G.V. Dolgushin, L.I. Larina, T.N. Komarova and V.A. Lopyrev, *Arkivoc*, 2003, **13**, 119-124.
- [18] G. M. Sheldrick, *Phase annealing in SHELX-90: direct methods for larger structures*, *Acta Crystallogr., Sect. A: Found. Crystallogr.*, 1990, **46**, 467.
- [19] G. M. Sheldrick, *SHELXL-97, Program for Crystal Structure Refinement*, Universität Göttingen, Göttingen, 1997.
- [20] P. V. Sluis and A. L. Spek, *Acta Crystallogr., Sect. A: Found. Crystallogr.*, 1990, **46**, 194.
- [21] M. T. Aroz, M. C. Gimeno, M. Kulcsar, A. Laguna and V. Lippolis, *Eur. J. Inorg. Chem.*, 2011, 2884–2894.
- [22] G. Roy and G. Mugesh, *J. Am. Chem. Soc.*, 2005, **127**, 15207-15217.
- [23] E. D. Glendening and J. A. Hrabal II., *J. Am. Chem. Soc.*, 1997, **119**, 12940-12946.

